J Mater Sci (2007) 42:8251–8253
DOI 10.1007/s10853-007-1724-5

Microstructure of laser-induced combustion synthesis of $Cu_{59.6}Zr_{36.9}Al_{3.5}$ alloy

Yanfang Wang · Zhide Han · Peng Zhong

Received: 7 January 2007 / Accepted: 26 March 2007 / Published online: 19 June 2007

Abstract $Cu_{59.6}Zr_{36.9}Al_{3.5}$ alloy are prepared by laser-induced combustion synthesis technology. The microstructure and phases formed of the product is studied by XRD and TEM. The product consists of mixtures of amorphous and crystalline phases, mainly(α-Zr, Zr_2Cu, $Zr_{10}Cu_7$ and Cu_8Zr_3. The amorphous and nanocrystalline phases content over 50% in volume estimated from the broad peak in the XRD spectrum. TEM and HRTEM results show that the microstructure is characterized by inhomogeneously distributed amorphous, nano Zr_2Cu, relatively gross (~100 nm) Zr_2Cu, and large grain $Cu_{10}Zr_7$.

Introduction

Combustion synthesis represents a promising method for the synthesis of advanced materials, such as ceramic-composites and intermetallic compounds. Combustion synthesis reactions are characterized by high combustion temperature (2,300–3,800 K), fast burning velocity (0.01–2 m/s) and heating rate (10^3–10^6 K/s). The rapid heating and rapid cooling associated with the combustion synthesis may produce metastable states in the products, such as amorphous and quasicrystalline phases [1]. Hence, this conventional method seems to be applicable to produce amorphous alloys. Laser-induced combustion synthesis (LCS) technique has been successfully applied to fabricate amorphous-containing alloys in Zr-based Zr–Al–Ni–Cu and Zr–Al–Ni–Ti quaternary alloy systems [2–4]. In the present work, we report on an investigation of the LCS of Cu–Zr–Al alloy.

Extensive attention has been paid to the Cu–Zr–Al alloys due to their high glass forming ability combined with good mechanical properties as well as relative low material cost [5–7]. The $Cu_{59.6}Zr_{36.9}Al_{3.5}$ alloy, which can form 3 mm bulk metallic glasses by suction casting [8], is a typical glass-forming system satisfying the combustion synthesis requirement. The negative enthalpies of mixing exist in binary Zr–Cu (–23 kJ/mol), Zr–Al (–44 kJ/mol) and Al–Cu (–1 kJ/mol) alloys [9].

Experimental

Elemental powders of Cu, Zr and Al (mesh 200–300, purity >99.00%) are mixed according to the stoichiometry. The homogeneously mixed powders are compacted into cylindrical green body with a diameter of 6 mm and a height of 5 mm. The specimen is mounted into a vacuum chamber, in which high-purity argon is continuously supplied to provide an inert environment. A high-energy HL-1500 CO_2 laser generator is employed to ignite the combustion synthesis reaction. The laser is operated at an output power of 800 W, beam diameter 6 mm and ignites time 5 s. Figure 1 shows the Macro-morphology of the green body and the LCS product. The product is sphere with smooth outer surface and metallic luster.

Y. Wang (✉)
Department of Materials Science and Engineering, China University of Petroleum (East China), Dongying, Shandong 257061, P.R. China
e-mail: wang_laser@yahoo.com.cn

Z. Han · P. Zhong
School of Physics Science and Technology, China University of Petroleum (East China), Dongying, Shandong 257061, P.R. China

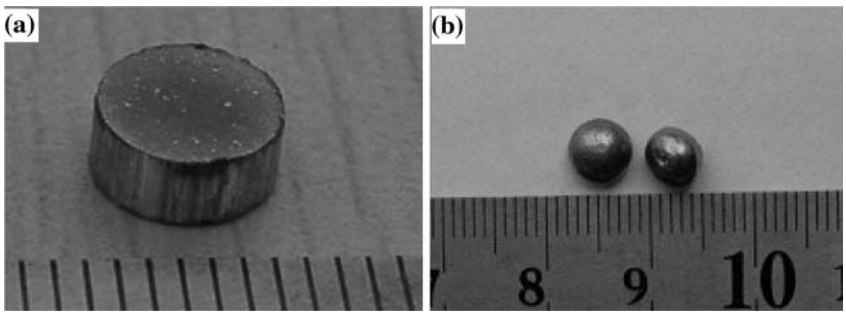

Fig. 1 Macro-morphology of the LCS products, (**a**) a green body; (**b**) LCS products

X-ray diffraction (XRD) is carried out for the phase identification with Cu K_a irradiation ($\lambda = 0.154060$ nm). The microstructure of the products is further characterized with a Tecnai G^2 20 high-resolution transmission electron microscope (HRTEM). The HRTEM specimens are prepared by standard twin-jet electrolytic thinning method in HNO_3–$C_3H_8O_3$–CH_3O electrolyte (volume ratio 5:2:13).

Results and discussion

Figure 2 shows the X-ray diffraction pattern of the LCS products. The process parameters are: laser power 800 W, beam diameter 6 mm, and ignite time 3 s. A broad diffraction peak appearing at $2\theta = 35$–$45°$ indicates the presence of an amorphous phase. However, sharp peaks due to crystalline phases are also present. The major crystalline phases are Zr_2Cu, $Cu_{10}Zr_7$, Cu_8Zr_3 and α-Zr. The area of the broad peak is indicative of the amorphous and nanocrystalline phase content. Amorphous phase is over 50% in volume as estimated from the area of the broad peak.

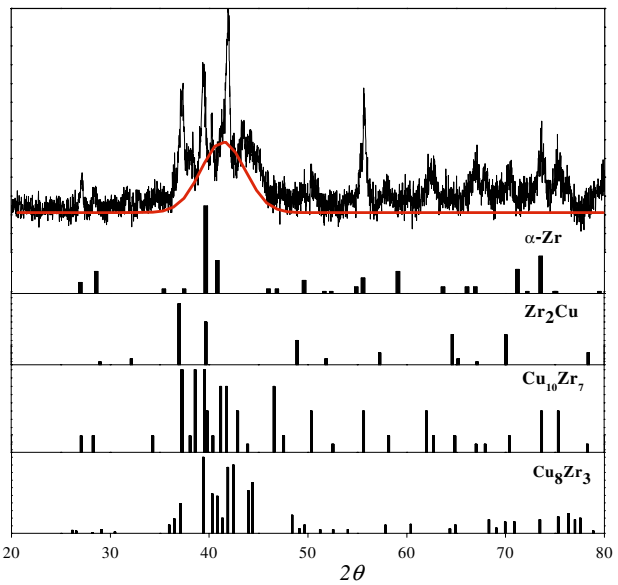

Fig. 2 X–ray diffraction spectrum of the LCS $Cu_{59.6}Zr_{36.9}Al_{3.5}$ alloy

To have a deeper knowledge of the LCS products, a detailed investigation is carried out using TEM and HRTEM. Figure 3 shows typical TEM and HRTEM images from the LCS $Cu_{59.6}Zr_{36.9}Al_{3.5}$ product. Figure 3a is a bright field image and its corresponding selected area diffraction (SAD). The broad diffraction halo rings together with sharp diffraction rings show the coexistence of nano body-centered tetragonal Zr_2Cu crystals embedded in an amorphous matrix. There are also relatively gross Zr_2Cu grains slightly larger than 100 nm, as can be seen from the bright field image. There is also pure amorphous areas, where diffuse halo rings are observed (b). The HRTEM image (c) together with the corresponding SAD pattern (d) show that the amorphous phase does exist but there are also fine rings from nano Zr_2Cu and sharp spots from gross $Cu_{10}Zr_7$. Two sets of SAD patterns from the α-Zr and $Cu_{10}Zr_7$ phases are shown in Figs. 4 and 5, in confirmation of the XRD result, but the Cu_8Zr_3 phase is not found, probably due to its small volume fraction. Thus the microstructure is characterized by inhomogeneously distributed amorphous, nano Zr_2Cu, relatively gross (~100 nm) Zr_2Cu, and large grain $Cu_{10}Zr_7$.

Conclusions

$Cu_{59.6}Zr_{36.9}Al_{3.5}$ alloy is prepared by laser-induced combustion synthesis technology. The product mainly consists of amorphous, α-Zr, Zr_2Cu, $Zr_{10}Cu_7$ and Cu_8Zr_3. The amorphous and nano-crystalline phases content over 50% in volume is obtained as estimated from the area of the broad peak in the XRD spectrum. Crystalline phases tI-Zr_2Cu, α-Zr and oC-$Cu_{10}Zr_7$ phases are identified both by TEM and XRD. TEM and HRTEM results show that the microstructure is characterized by inhomogeneously distributed amorphous, nano Zr_2Cu, relatively gross (~100 nm) Zr_2Cu, and large grain $Cu_{10}Zr_7$.

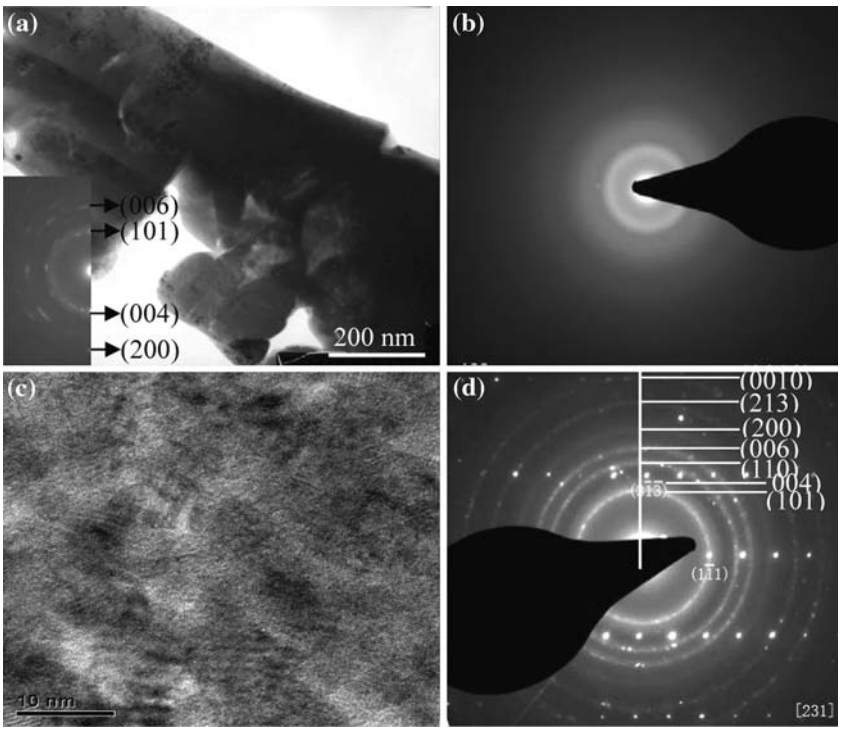

Fig. 3 TEM and HRTEM images of LCS $Cu_{59.6}Zr_{36.9}Al_{3.5}$ product (**a**), bright field image and corresponding SAD pattern, identified as Zr_2Cu, (**b**), SAD of the amorphous phase, (**c**), HRTEM image showing nano Zr_2Cu precipitates, (**d**), SAD pattern, identified as nano-crystalline Zr_2Cu and [231] $Cu_{10}Zr_7$

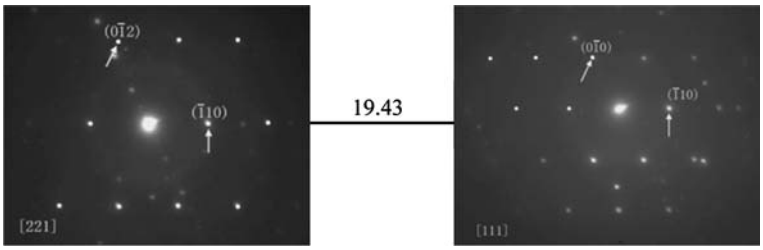

Fig. 4 SAD patterns of the α-Zr phase (the tilting angles between neighboring patterns are marked). The background diffuse ring is from the amorphous phase

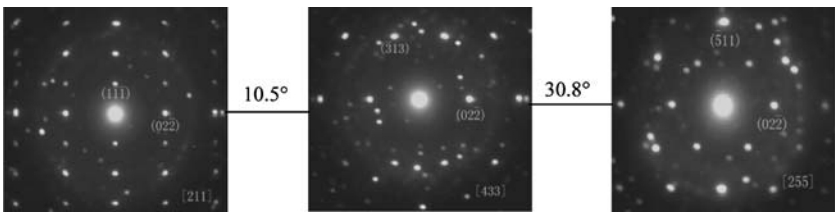

Fig. 5 SAD patterns of the $Cu_{10}Zr_7$ phase (the tilting angles between neighboring patterns are marked). The background diffuse ring is from the amorphous phase

References

1. Moore JJ, Feng HJ (1995) Prog Mater Sci 39:243
2. Wang CS, Gao LH, Li G, Wang YF, Xia YL, Bysakh S, Dong C (2003) J Mater Sci 38:1377
3. Wang CS, Wang YF, Gao LH, Li G, Xia YL, Dong C (2004) J Non-Cryst Solids 334–335:513
4. Wang YF, Wang CS, Pan XM, Dong C (2005) Mater Lett 59:2574
5. Inoue A, Zhang W (2002) Mater Trans 43:2921
6. Inoue A, Zhang W, Zhang T, Kurosaka K (2001) Acta Mater 49:2645
7. Inoue A, Zhang W, Zhang T, Kurosaka K (2002) J Non-Cryst Solids 304:200
8. Wang Q, Wang YM, Qiang JB, Zhang XF, Shek CH, Dong C (2004) Intermetallics 12(10–11):1229
9. Takeuchi A, Inoue A (2000) Mater Trans, JIM 41(11):1372